A DATABASE OF DEEP SEISMIC SOUNDING PEACEFUL NUCLEAR EXPLOSION RECORDINGS FOR SEISMIC MONITORING OF NORTHERN EURASIA

Igor B. Morozov,[1] Scott B. Smithson,[1] Elena A. Morozova,[1] and Leonid. N. Solodilov[2]

University of Wyoming[1]; Center CEON, Moscow, Russia[2]

Sponsored by Defense Threat Reduction Agency

Contract No. DSWA01-98-1-0015

ABSTRACT

The database of seismic recordings of Peaceful Nuclear Explosions (PNEs) at the University of Wyoming now includes 19 PNEs recorded along 7 long-range refraction/reflection profiles: QUARTZ, CRATON, KIMBERLITE, RIFT, METEORITE, and two lines of project RUBY. The data from RUBY also include recordings of two Kazakhstan nuclear tests. This grid of reversed profiles (also with fan recoding for RUBY) covers the East European Platform, the Ural Mountains, the West Siberian Platform and the Siberian craton, and the Baikal Rift. Dense, 3-component, short-period recordings along these profiles provide practically the only reliable source of seismic information for seismic calibration of these vast aseismic regions. These recordings offer unique opportunities to study propagation effects of regional seismic phases, to examine their correlation with geologic and tectonic features, and to develop new constraints on the structure of the crust and upper mantle.

We are delivering databases of travel-time, spectral, and amplitude attributes of *P*, *S*, and *Lg* phases from PNE recordings. Dense observations of these phases at about 10- to 20-km spacings allow unusual, nearly continuous representation of the variations of their spectral properties over about 0- to 3200-km propagation ranges. Our preliminary analysis has uncovered numerous indications of strong *Lg* and other regional phases variability within the region. In order to increase robustness and versatility of the database, we provide spectral data in several forms, including the traditional (Fast Fourier Transform), multi-taper, and multi-component spectra.

We summarize our recent findings from the analysis of PNE arrivals in Northern Eurasia. These results include (1) unusually detailed velocity and attenuation structure of the crust and uppermost mantle, (2) characterization of crustal attenuation through coda measurements, (3) constraints on seismic scattering, and (4) detailed imaging of the crustal basement using receiver functions. All of these factors are of primary importance for modeling of crustal guided phases, such as the P_g and L_g. We discuss further possible extensions of this database, including a simple empirical technique for regionalization of seismic travel times and for building the source-specific station corrections for a large part of Northern Eurasia. With further analysis facilitated by the developed database, travel-time, amplitude and waveform information from PNE records will provide valuable quantitative constraints and realistic structural data for modeling of L_g and other regional phases, contributing to the development and calibration of regional seismic discriminants.

KEY WORDS: Russian Eurasia, Peaceful Nuclear Explosions, regional seismic phases

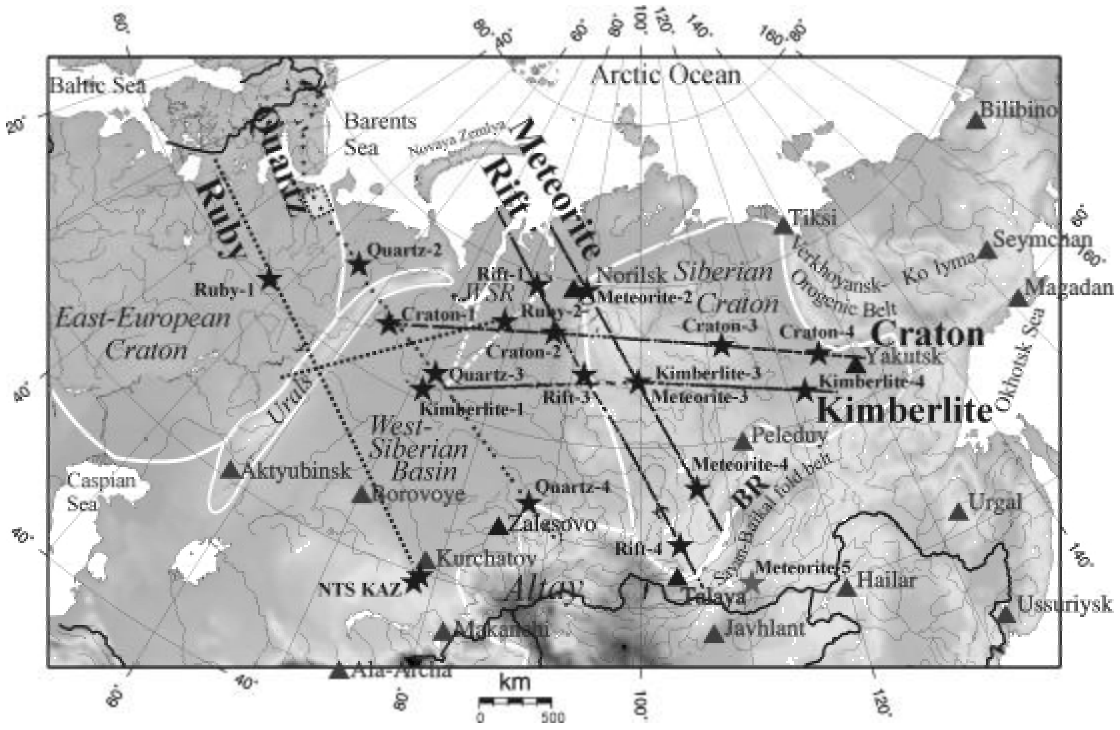

Figure 1. DSS PNE profiles under study at the University of Wyoming: QUARTZ, CRATON, KIMBERLITE, RIFT, METERORITE, and RUBY (two lines, obtained recently). Large stars are the PNEs; small stars (for profile QUARTZ only) are the chemical explosions. Profile RUBY is shown schematically. The coordinates and other parameters of the PNEs used in these profiles were reported by Sultanov et al (1999). White contours show the major tectonic units (labeled: WSR – West Siberian Rift, BR – Baikal Rift). Note the extent of systematic, continuous profiling, with PNEs detonated at the intersections of the 3000- to 4000-km-long profiles. The profiles are close to some of the IMS stations (labeled triangles). The profile QUARTZ has been studied extensively for the upper mantle and crustal structure, for seismic coda effects and crustal reverberations. The box NW of PNE QUARTZ 2 indicates the area where crustal attenuation was measured using coda amplitude analysis.

OBJECTIVE

In cooperation with Center GEON, Moscow, Russia, the University of Wyoming has obtained a substantial part of the unique Deep Seismic Sounding (DSS) data including systematic and continuous profiling of Peaceful Nuclear Explosions (PNEs) in Northern Eurasia (Figure 1). Along with reversed recording of the PNEs to over 3000-km ranges, 30 to 80 chemical explosions were recorded in each of the ultra-long profiles (Figure 1), making these datasets unparalleled in terms of both detailed coverage of the crust and upper mantle and also as comprehensive collections of seismic recordings of explosions at regional distances.

In this study, these unique seismic data are being investigated for their potential use in nuclear explosion monitoring. The importance of this research is emphasized by the great variety of the tectonic structures covered by the profiling and also by the fact that DSS recordings cover largely aseismic regions of Northern Eurasia where virtually no other data are available for seismic calibration (Figure 1). The DSS data sets contain abundant 3-component recordings of the full spectrum of regional phases that can be used in seismic calibration and discrimination.

RESEARCH ACCOMPLISHED

The discussion below can be separated into three inter-related main lines:

1. Analysis of the crustal and upper mantle structure and its effects on the propagation of seismic phases. This includes unusually detailed imaging of the velocity and attenuation structure of the crust and upper mantle and constraining of scattering properties of the crust, and development of approaches that could take advantage of the unusual properties of the DSS PNE data sets.
2. Characterization of seismic phases from the PNEs and assembling a database of parameters of these phases in a form suitable for nuclear explosion monitoring. This effort is focused on uniform treatment of the entire PNE data set and preparing grounds for regionalization of seismic discriminants computed from the different profiles.
3. As a first step of the advanced analysis in (2), empirical regionalization (at present, by interpolation) of the seismic attributes observed in different profiles and by relating these attributes to regional tectonics and to the structures revealed by seismic observations

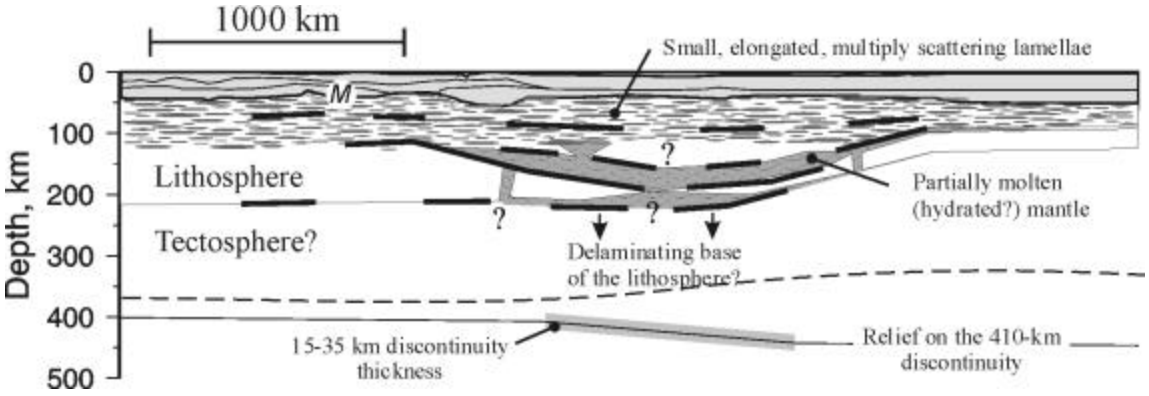

Figure 2. A collage of the recent models of the uppermost mantle derived from controlled-source seismic investigations in Northern Eurasia. The lithosphere varies in thickness between 120-220 km (Morozova et al, 1999), with significantly higher velocity than in the IASP91 model, three groups of reflecting boundaries (bold lines), and potential regions of mechanical instability of its base (Morozov et al, 1998b). The upper about 80 km[1] of the lithosphere are pervasively heterogeneous, modeled as stochastic medium with about 0.5-km vertical correlation length, ±2% to 5% velocity fluctuations, and aspect ratio of up to 50-100 (Ryberg et al, 2000; A. Ryberg and Wenzel, 1999; A. Gorman et al, in review). Due to such strong heterogeneity, seismic waves at frequencies above 5 Hz do not penetrate below this layer but form "high-frequency scattering waveguide" (SWG) modes propagating through it by means of multiple scattering[2] (Tittgemeyer et al, 1996; Ryberg and Wenzel, 1999). Below about 100-120 km, seismic scattering and increased attenuation suggest a layer of partial melting, probably initiated by the presence of fluids (Thybo and Perchuc, 1997; Morozov et al, 1998b; Nielsen et al, 1999). Both of these scattering layers are often viewed as typical in a continental lithosphere (Enderle et al, 1997; Tittgemeyer et al, 1999b; Thybo and Perchuc, 1997). An analysis of topside reflections from the transition zone discontinuities suggests their gradational character and about 20-30 km relief of the 410-km discontinuity (Priestley et al, 1994; Morozova et al, 1999).

In recent years, due to increased availability of the DSS PNE profiles, the **heterogeneity of the crust and upper mantle**, and particularly of the continental lithosphere, has been convincingly documented. Wide-angle refraction,

[1] 100-120 km in a recent 2-D modeling by Ryberg et al (2000).

[2] Probably a better name for such mantle structure would be a “diffusive screen.”

reflection, receiver function, and attenuation studies revealed strong velocity gradient and reflecting boundaries within the continental lithosphere, with broad zones containing pockets of partial melts, topography and gradational character of the transition zone discontinuities (Figure 2). Of particular importance for regional phase propagation are the abundant reflecting boundaries within about 60-150 km below the Moho and the pervasive, strong (±2-5% in velocity), small-scale ($a_z \approx 0.5$-2 km, $a_x \approx 10$-20 km) heterogeneity of the uppermost mantle (Figure 2) recently suggested from investigations of short-period seismic scattering (Ryberg et al, 1995). If confirmed, these findings could overturn both the existing petrophysical models of the upper mantle, and our understanding of the very nature of the upper-mantle seismic phases (*Pn*, *P*, *Sn*, *S*) used as the basis for nuclear test discrimination (e.g., Tittgemeyer et al, 2000). It appears that the present understanding of seismic wave propagation within the uppermost mantle is still limited and far from being mature. Predictions of *Pn* amplitudes in structures like the one shown in Figure 2 can vary by orders of magnitude and be frequency dependent, requiring sets of "source-specific amplitude corrections" for computing discriminants. Notably, for many years to come, the DSS PNE data will still represent by far the most comprehensive and insightful datasets for testing the hypotheses of short-period regional wave propagation and calibrating the discrimination models.

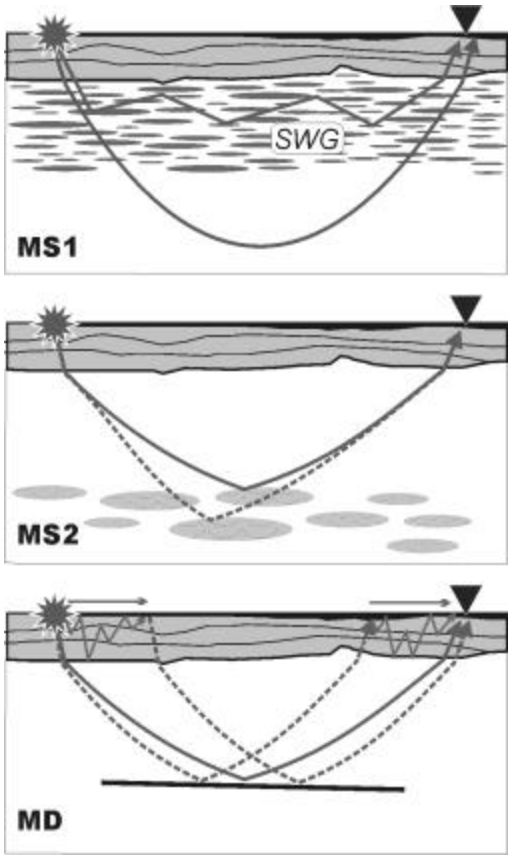

Figure 3. Three competing models of seismic scattering observed in the records from long-range refraction profiles (Figure 1): MS1: strongly scattering mantle lid; high-frequency phases reach the receivers by a diffusive scattering-waveguide (SWG) propagation (blue ray), the phases penetrating deeper lose their high-frequency energy in this layer (red ray) (Ryberg et al, 1995); MS2: the upper 80 km of the mantle is relatively transparent, single scattering occurs (possibly) on pockets of partial melt between 120-200 km; this scattering is causes an increased complexity of the first arrivals (Thybo and Perchuc, 1997); MD: the observed coda is mainly due to crustal scattering at both source and receiver ends, the mantle is "deterministic" in the sense that possible mantle scattering layers may be resolved only as apparent reflecting boundaries (Morozov and Smithson, 2000).

Until recently, PNE records were analyzed primarily with an emphasis on travel-time modeling and inversion. In this study, we switch our attention on the amplitude and waveform pattern of the PNE wavefield. By challenging the broadly accepted view of a relatively featureless upper mantle, amplitude patterns of PNE recordings make a strong impact on our understanding of wave propagation through the uppermost mantle. However, no consistent theory of the scattering and attenuation properties of the uppermost mantle was established, and the models that have been put forward often contradict each other.

A well-known controversy of this kind is the explanation of is the long-range (~2000-3000-km) *Pn* phase observed in the records from profiles QUARTZ and RUBY (Ryberg et al, 1995). Frequency content of this phase is leading to fundamental conclusions about the fine-scale structure of the upper half of the lithosphere (Figure 2). *Pn* in the $f < 5$ Hz, band is largely described by ray theory, whereas for $f > 5$ Hz, the signal appears significantly more complex.

Ryberg et al (1995) interpreted this frequency separation of the long-range *Pn* as an indication of a strongly scattering uppermost mantle, with ±5% RMS velocity fluctuations[3] having ~0.5- to 2-km vertical correlation length and a Gaussian-like spatial correlation function (Figure 3, top; Ryberg and Wenzel, 1999). However, Morozov (in press) argued that there was *no* such frequency separation, and Morozov et al (1998a,b; Morozov and Smithson, 2000) showed that a whispering-gallery (WG) model of this phase, based on a mantle velocity gradient, reflectivity, and crustal scattering could give a better explanation for the observed wavefield and could also help constrain details of the lithospheric structure. Independently of this discussion, Thybo and Perchuc (1997) and Nielsen et al (1999, and two papers in review) analyzed perturbations of the first arrivals from explosions between the offsets of 800 – 1400 km and suggested a source of scattering below about 100 – 140 km within the mantle (Figure 3, middle) in general agreement with the findings by Morozov et al (1998b). Similar models of mantle scattering were also derived from the North American Deep Probe data (Gorman et al, in review); nevertheless, these models were also criticized for their disregard of crustal scattering (Morozov and Smithson, 2000).

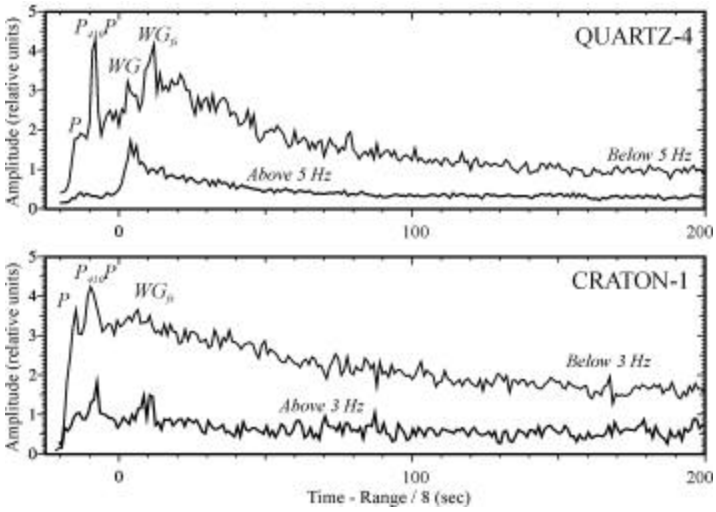

Figure 4. Amplitude of the high-frequency and low-frequency (filter corner frequency is 5 Hz for QUARTZ and 3 Hz for CRATON) records within the offset range 2500 - 2600 km from PNE QUARTZ-4 and CRATON-1 (modified from Morozov and Smithson, in press). Time reduction is 8 km/s, and 7 three-component instantaneous trace amplitude records were averaged within a 2-s sliding time window and within the offset range (Morozov and Smithson, 1996) was used. First arrivals, a reflection from the 410-km discontinuity, and two whispering-gallery phases (*WG* and WG_{fs}) are indicated. Note the difference of the codas following the free-surface multiple refraction WG_{fs} at low frequencies and the Moho multiple *WG* at high frequencies. Note the about 150-sec-long codas following the arrivals; also note the differences in these codas between the high- and low-pass filtered records.

Crustal scattering, however, appears to be a primary factor in the observed PNE wavefield (Figure 3, bottom; Morozov and Smithson, 2000). Crustal $Q_P \approx 270 \cdot f^{0.3}$ accounts for the frequency-dependent codas following the PNE arrivals at about 2500 km from the PNE QUARTZ-4 (Figure 4), confirming our association of the PNE coda effects with crustal, preferably $P \rightarrow L_g$ or $L_g \rightarrow P$ scattering (Singh and Herrmann, 1983; Dainty, 1990). Such comparatively low values of *Q* might be related to the effect of the thick sedimentary cover of the Pechora basin sampled by the part of the profile used in this analysis (Morozova *et al*, 1999). Figure 4 also shows that the two whispering-gallery (*WG*) multiples forming the long-range P_n are clearly distinct in the character of their codas. The first, Moho multiple labeled *WG* in Figure 4 is followed by a coda that dominates the high-pass filtered record. However, in the low-frequency band, the strongest phase is the free-surface P_n multiple (WG_{fs}) followed by its coda. The higher amplitude of the WG_{fs} event is consistent with higher reflectivity of the free surface compared to the Moho. The longer and low-frequency coda of WG_{fs} suggests a predominance of surface waves that propagate efficiently at lower frequencies and are progressively more attenuated as the frequency increases; this observation points again to a crustal origin of the coda. Moreover, the coda decay rates for QUARTZ-4 and CRATON-1 appear to be different

[3] This estimate was recently reduced to ±2% variations, but with a thicker scattering layer (100-120 km), based on 2-D simulations (Ryberg et al, 2000). However, this new modelling is still based on unrealistic, featureless upper crust, and does not take into account the high-velocity, high-gradient upper mantle under the East European Platform that is strongly different from the upper mantle in Siberia and from the global average.

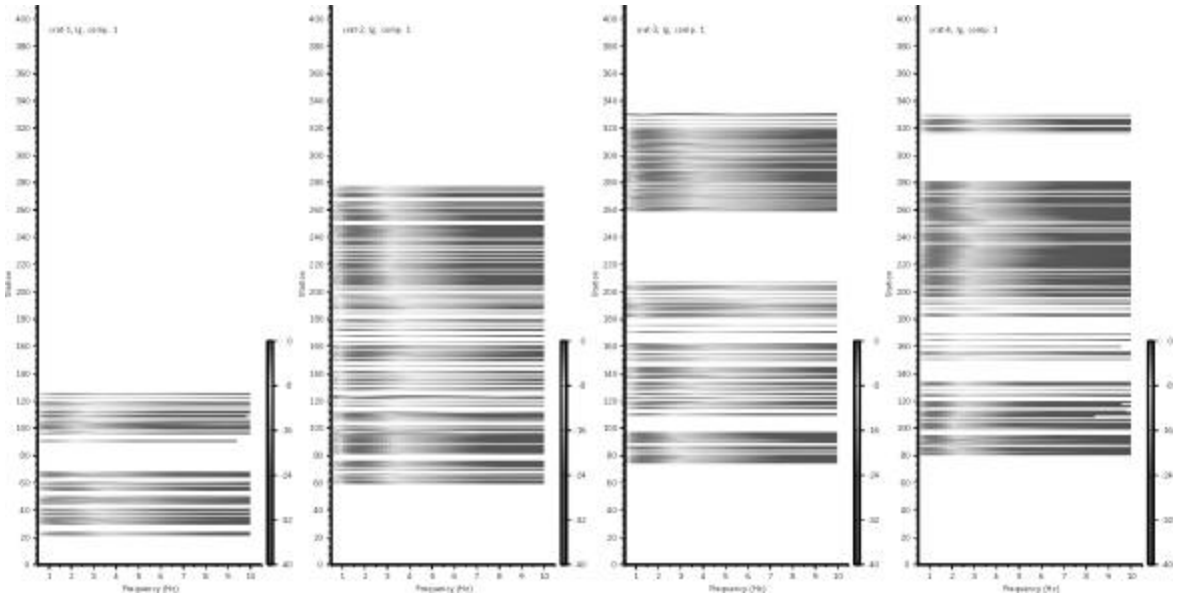

Figure 5. Lg spectra from the four CRATON PNEs from individual recording stations and for the inline component of recordings. Gray-shade levels correspond to the amplitude levels below the RMS values within the same windows, in dB.

indicating a variation in crustal properties along the profiles (Figure 1); this difference will be quantified in a detailed study in the future.

With much more DSS PNE data available for analysis than before, **a database of amplitude and spectral parameters** derived in a uniform manner is required. Such a database is being built at present using a set of approaches and tools designed in our analysis of the QUARTZ data set. The attributes stored in this database include:

1. Travel times of the *S* waves and *Lg* picked from the PNE sections.
2. Instantaneous amplitude envelops of the individual components and 3-component instantaneous polarization vectors of the corresponding windowed arrivals (Morozov and Smithson, 1996). The 3-component amplitude measures produce amplitude estimates that are more stable in respect to near-receiver scattering (Kennett, 1993).
3. Spectra of the *P*, *S*, and *Lg* waves. We provide both Fast Fourier Transform (FFT) spectra and smoothed, multiple taper spectra (Atkinson and Mereu, 1992). The multiple taper spectra are known to provide statistically stable spectral estimates. Both types of spectra are computed for all three individual components of ground motion and for 3-component amplitudes, thereby further increasing their stability (Figure 5).
4. Estimates of pre-shot and end-of-the-record noise (>300-sec after the first arrivals). These are measured using the same amplitude and spectral estimators as applied to event windows.

We expect that this database will serve as a primary source of data for discrimination studies using these PNE data before the full records become broadly available[4]; however, even after that, the database would provide useful additional attributes that can be directly used in computing seismic discriminants.

Utilizing high density and large number of recordings, the spectral data can be presented not only in its conventional form, as spectra recorded at the individual channels (Figure 5), but also as a nearly continuous spectrogram of the

[4] With funding provided by DTRA and NSF, full PNE and chemical explosion records from 9 DSS long-range projects including all of those shown in Figure 1 will become broadly available through IRIS DMC within the next four years.

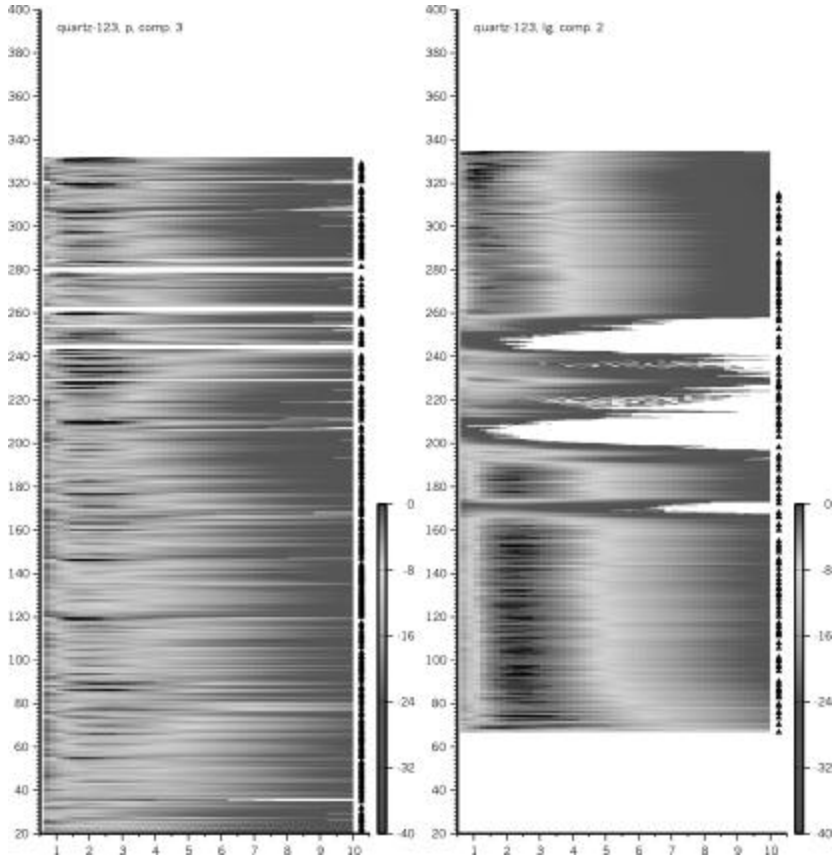

Figure 6. Three-component spectrograms for *P*-wave and *Lg* waves from PNE QUARTZ-2. The triangles on the right of each of these plots indicate the starts of the event windows used for spectral analysis. For each of these windows, a spectrogram was built using multiple Butterworth filtering. Because of the high density of the records, the resulting spectrograms overlap in time, resulting in a nearly continuous, time-frequency representation of wave propagation.

entire wave propagation (Figure 6). Such representation of wave propagation might be particularly useful for comparisons with numerical modeling, which is planned for a future study.

Uniform geographic coverage of the profiles crossing a broad range of tectonic provinces suggests **direct methods of seismic regionalization**. The existing empirical (as opposed to model-based) travel-time regionalization techniques usually rely on (1) classification of the target region in terms of tectonic provinces; (2) assignment of a single regional travel-time curve (TTC) to each of these provinces; (3) using an heuristic interpolation formula to interpolate between these 1-D TTCs when the source and receiver are located in different regions. Although this procedure is simple and robust, offering an efficient way to interpolate between a few 1-D TTCs, its greatest weakness lies in propagation of constant shallow velocity structures across vast regions. In contrast, dense DSS recordings result in numerous high-quality first-arrival TTCs associated with the areas of Northern Eurasia (Figure 1), and we can formulate a regional *P*-wave travel-time model honoring the regional variability of the travel times.

To derive a regional travel-time model, we perform direct spatial interpolation of the travel-time data, also employing heuristic interpolation rules. Interpolation is performed within common-offset sections, and therefore our regionalization is offset-dependent. For any given source-receiver offset, each travel-time pick is associated with the corresponding source-receiver midpoint, and the travel times are interpolated between these midpoints, resulting in a common-offset travel-time field (Figure 7). Computed for a range of offsets, these travel-time fields form a 3-D travel-time cube in latitude/longitude/offset space comprising our regional first-arrival travel-time model. Note that

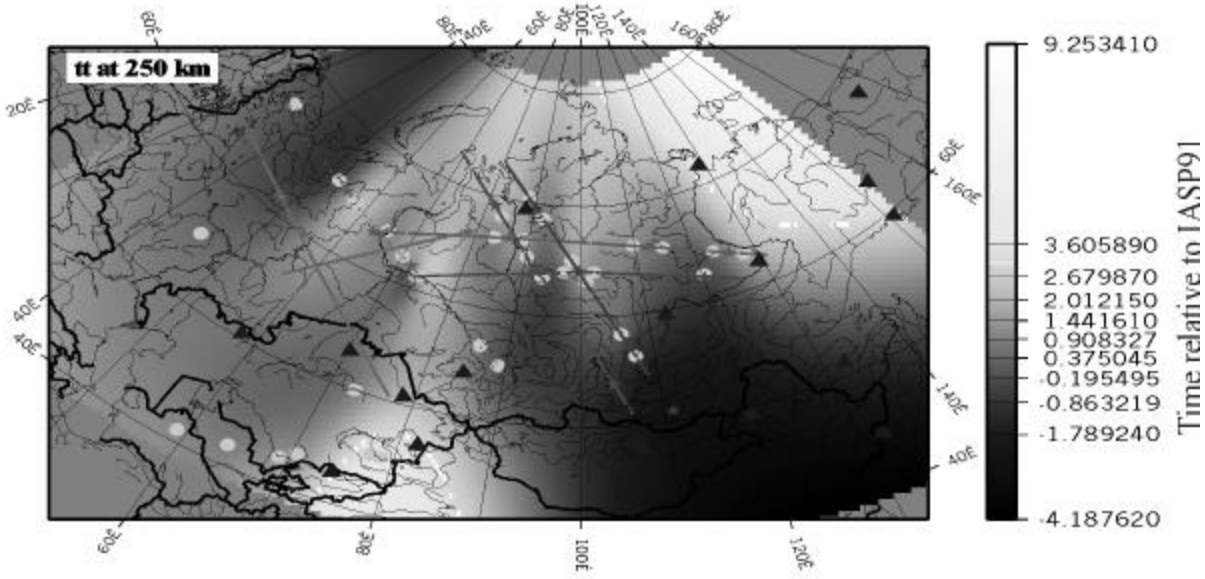

Figure 7. Interpolated travel-time field for offset equal 250 km from DSS travel-time picks. The travel-time data used here include the first-arrival travel times from the PNEs (without RUBY) and from published DSS interpretations of regional DSS profiles, primarily in Kazakhstan (compiled by V. Khalturin, personal communication). Gray dots indicate the positions of the midpoints. A set of similar surfaces built for a range of offsets forms a 3-D travel-time cube that can be used as a regional travel-time model. Black triangles indicate the IMS stations.

such regionalization is more detailed at shorter offsets; in particular, the zero-offset travel-time section corresponds to station statistics.

For a selected station location, by making a conical slice through this travel-time cube, we obtain predicted travel times from any point within the region to that station. These predicted travel times form the source-specific station correction (SSSC) that can be used in station calibration; Figure 8 shows such a surface for a station at Borovoye in Kazakhstan. An advantage of such a way of obtaining SSSCs is in its straightforward manner, its ability to build a correction surface for any location, and on its honoring the observed regional travel times rather than the IASP91 model (which is known to be grossly unsatisfactory at regional distances in Northern Eurasia). With an inclusion of the travel-time picks made at the station, the SSSC can be further improved.

In future research, we plan to improve the above interpolation procedure in several ways: (1) by reducing propagation of the near-offset travel-time perturbations (caused by the near-source and near-receiver structures) to large offsets; (2) by introducing a stochastic mechanism of error estimation; (3) by extension of the procedure to mapping other attributes, such as the values of seismic discriminants.

CONCLUSIONS AND RECOMMENDATIONS

1. DSS studies of the ultra-long-range profiles have demonstrated strong crustal and upper mantle heterogeneity that may be of primary importance for explaining the amplitudes and spectra of regional phases used in seismic monitoring.
2. The database of amplitude and spectral attributes of the seismic phases from 19 PNEs recorded in 7 ultra-long refraction profiles would provide a comprehensive source of information for regionalization of *Lg*, *P*- and *S*-wave, and crustal scattering properties in Northern Eurasia.
3. Joint analysis of the data from the entire PNE dataset results in a straightforward, empirical scheme of travel-time regionalization that can be extended to regionalization of seismic discriminants.

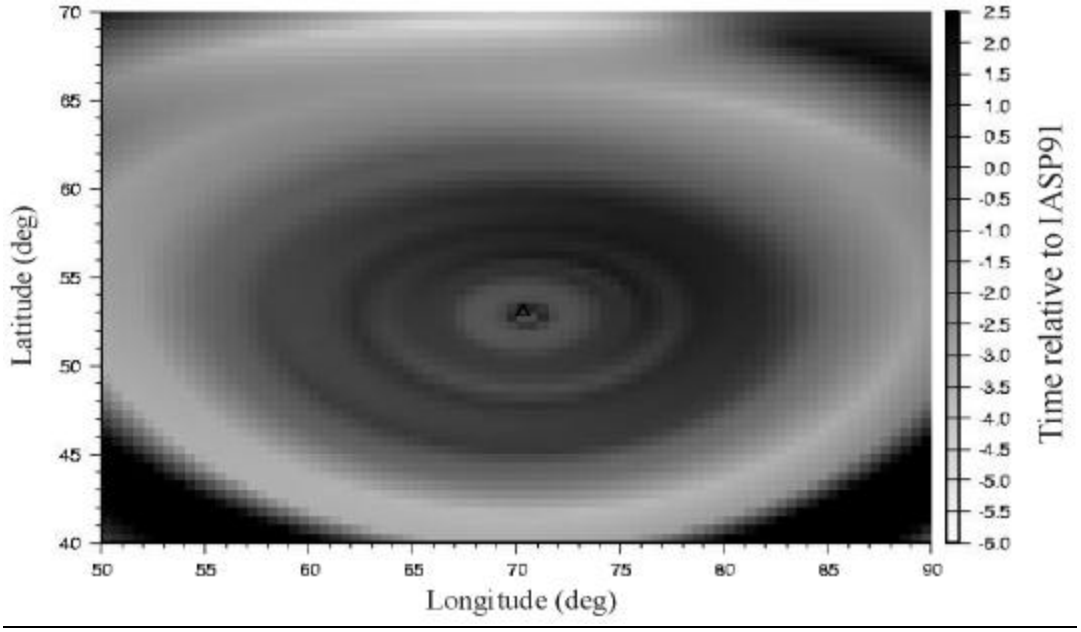

Figure 8. Preliminary source-specific station correction surface for station at Borovoye, Kazakhstan, extracted from the 3-D travel-time cube illustrated in Figure 7.

REFERENCES

Atkinson, G. M., and R. F. Mereu (1992), The shape of ground motion attenuation of curves in Southeaastern Canada, Bull. Seism. Soc. Am., 82, 2014-2031.

Dainty, A. M. (1990), Studies of coda using array and three-component processing, PAGEOPH, 132, 221-244.

Gorman, A.R., R.M. Clowes, R.M. Ellis, T.J. Henstock. G.D. Spence, G.R., Keller, A.R. Levander, C.M. Snelson, M.J.A. Burianyk, E.R. Kanasewich,, I. Asudeh, Z. Hajnal and K.C. Miller (2001). Deep Probe - Imaging the roots of western North America. Canadian Journal of Earth Sciences. In review.

Kennett, B. L. N. (1993), The distance dependence of regional phase discriminants, Bull. Seismol. Soc. Am., 83, 1155-1166.

Kennett, B. L. N. (1987), Observational and theoretical constraints on crustal and upper mantle heterogeneity, Phys. Earth Planet. Interiors, 47, 319-332.

Morozov, I. B. (2001), Comment on "High-frequency wave propagation in the uppermost mantle" by T. Ryberg and F. Wenzel, J. Geophys. Res., in press.

Morozov, I. B., and S. B. Smithson (1996), Instantaneous polarization attributes and directional filtering, Geophysics, 61, 872-881.

Morozov, I., B., E. A. Morozova, and S. B. Smithson (1997), Observation of Lg and S wave propagation along the ultra-long profile "Quartz", Russia, in: Fuchs, K. (Ed.) Upper mantle heterogeneities from active and passive seismology, Kluwer, pp. 147-154.

Morozov, I., B., E. A. Morozova, and S. B. Smithson (1998a), On the nature of the teleseismic Pn phase observed in the recordings from the ultra-long profile "Quartz", Russia, Bull. Seism. Soc. Am., 88, 62-73.

Morozov, I., B., E. A. Morozova, S. B. Smithson, and L. N. Solodilov (1998b) 2-D image of seismic attenuation beneath the Deep Seismic Sounding profile QUARTZ, Russia, Pure Appl. Geoph, 153, 311-343.

Morozova, E. A., I. B. Morozov, S. B. Smithson, and L. N. Solodilov (1999), Heterogeneity of the uppermost mantle beneath the ultra-long range profile "Quartz," Russian Eurasia, J. Geophys. Res., 104 (B9), 20,329-20,348.

Nielsen, L., H. Thybo, and L. Solodilov (1999), Seismic tomographic inversion of Russian PNE data along profile Kraton, Geoph. Res. Lett., 26, 3413-3416.

Enderle, U., M. Tittgemeyer, M. Itzin, C. Prodehl, and K. Fuchs (1997), Scales of structure in the lithosphere - Images of processes, Tectonophysics, 275, 165-198.

Ryberg, T., and F. Wenzel (1999), High-frequency wave propagation in the uppermost mantle, J. Geophys. Res., 104, 10,655-10,666.

Ryberg, T., K. Fuchs, A. V. Egorkin, and L. Solodilov (1995), Observations of high-frequency teleseismic P_n on the long-range Quartz profile across northern Eurasia, J. Geophys. Res., 100, 18151-18163.

Ryberg, T., M. Tittgemeyer, and F. Wenzel (2000), Finite-difference modelling of *P*-wave scattering in the upper mantle, Geophys. J. Int, 141, 787-800.

Morozov, I. B., and S. B. Smithson (2000), Coda of long-range arrivals from nuclear explosions, Bull. Seism. Soc. Am., 90, 929-939.

Thybo H. and E. Perchuc (1997), The seismic 8º Discontinuity and Partial Melting in Continental Mantle, Science, *275*, 1626-1629.

Priestley, K. F., J. Cipar, A. Egorkin, and N. I. Pavlenkova (1994), Upper-mantle velocity structure beneath the Siberian Platform, Geophys. J. Int., 118 (2), 369-378.

Singh, S., and R. B. Herrmann (1983), Regionalization of crustal coda *Q* in the Continental United States, J. Geophys. Res., 88, 527-538.

Sultanov, D. D., J. R. Murphy, and Kh. D. Rubinstein (1999), A seismic source summary for Soviet Peaceful Nuclear Explosions, Bull. Seism. Soc. Am., 89, 640-647.

Tittgemeyer, M., F. Wenzel, K. Fuchs, and T. Ryberg (1996), Wave propagation in a multiple-scattering upper mantle—observations and modeling, Geophys. J. Int., 127, 492-502.

Tittgemeyer, M., F. Wenzel, T. Ryberg, and K. Fuchs (1999), Scales of heterogeneities in the continental crust and upper mantle, Pure and Applied Geophysics. 156, 1-2, 29-52.

Tittgemeyer, M., F. Wenzel, and K. Fuchs (2000), On the nature of *Pn*, J. Geophys. Res., 105, 16,173-16,180.